Advanced Journal of Chemistry-Section A, 2019, 2(2), 147-164
Research Article
http://ajchem-a.com

Mineralogy and Pollution Status of Columbite-Tin Ore Contaminated Soil

Adams Udoji Itodo *, Raymond Ahulle Wuana, Bulus Emmanuel Duwongs, Davoe Danbok Bwede

ARTICLE INFO

Received: 16 January 2019
Revised: 27 January 2019
Accepted: 28 January 2019
Available online: 9 February 2019

KEYWORDS

Pollution Index
Geo-Accumulation
Mineral
Soil
Columbite
Tin
Plateau

ABSTRACT

Mining activities are one of the numerous ways by which man impacts on his environment. In this study, two non-destructive analytical techniques (XRF and XRD) were employed in the mineralogical characterization of Columbite-Tin ore and their contaminated soils. This investigates associated unnoticed minerals as well as the impact of mining on vicinity farmland soils on the Yelwa-Mbar mining site, Nigeria. The chemical characterization of Columbite ore using electron dispersive XRF revealed that most of the Columbite mineral deposits in the Plateau mining sites contain Niobium mineral in various proportions and vary from deposit to deposit depending on the geochemical composition of the minerals that formed the parent rock. Tin content as determined by ED-XRF impart that the ore can be utilized directly in the furnace because of its high cassiterite content (85.43%). The percentage elemental composition of soil around the mining vicinity unveiled the presence of Radionuclides K-40, Rubidium and Thorium in the soil. This is of great concern. The XRD mineralogical investigation of Columbite shows the presence of associated braunite, cassiterite, ilmenite, quartz, and zircon while the phase pattern for Tin ore confirmed the availability of cassiterite, magnetite and litharge. Pollution status based on contamination factor and geo-accumulation indices gave both radionuclides and heavy metal concentrations that depicts moderate to extreme contaminations.

GRAPHICAL ABSTRACT

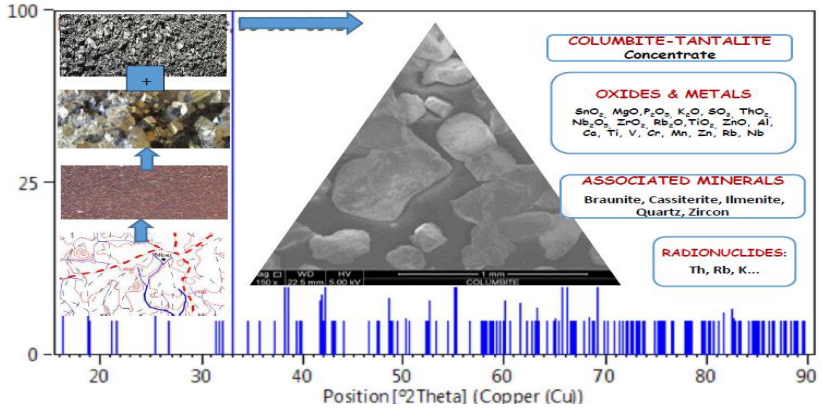

* Corresponding author's E-mail address: itodoson2002@gmail.com, Tel.: +02348039503463
Department of Chemistry, Federal University of Agriculture, PMB 2373 Makurdi, Nigeria.

Introduction

One of the ways by which man impacts on his environment (both natural and built) is through mining activities [1]. Mining in Nigeria started as far back as the eighteenth century. Over 500 occurrences and deposits of over different minerals are known so far to exist within the country with the exploration of some of them being on a small scale [2]. The mining industry generates wastes which contain high concentrations of metals and metalloids which contaminates agricultural soils, air and water. These pollutants can be mobilized, resulting in leaching into ground and surface water. Most of these heavy metals are highly toxic and are not biodegradable [3].

In Jos, Plateau State, Tin and allied metals mining started about 1902. Within this span of time the tin fields have been subjected to a process of unregulated mining activity, thereby devastate and depleted agricultural lands by intensive and extensive mechanized mining activities [4]. The early tin miners often overlooked the minerals of Niobium and Tantalum or had a great difficulty in separating them from the tin. Consequently, all cassiterite concentrates were contaminated with columbite-tantalite [4].

The contamination of agricultural soils and depletion of the environment as a result of unregulated mining activities poses threats to the environment and human. This research focus on the mineral characterization of Tin-Columbite contaminated soil. The study also investigates dearth information on the classes of contaminants and the compounds that are unearthed as a result of mining activities.

Sample Location and Site Description

Yelwa-Mbar (Figure 1) is in Bokkos local government of Plateau State Nigeria. Plateau state (latitudes 9° 51'30'N; 10° 02'00''N and longitudes 8° 48'00''E; 9° 59'00''E) is located in Nigeria's middle belt, with an area of 30,913 km^2 (11,936 sq m).

The state has an estimated population of about three million people. Named after the picturesque Jos, Plateau is a mountainous area in the north central of the state with captivating rock formations. Bare rocks are scattered across the grasslands, which cover the Plateau. The altitude ranges from around 1,200 meters (about 400 feet) to a peak of 1,829 meters above sea level in the Shere Hills range near Jos the state capital. It was noted [5] that plutonic and volcanic rocks predominate in the Jos Plateau, with some alluvium and other unconsolidated deposits. Years of tin mining have also left the area strewn with deep gorges and lakes.

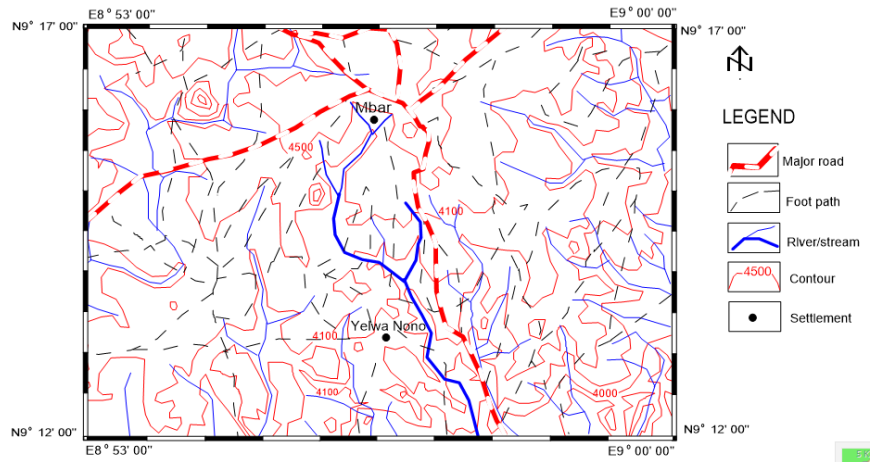

Figure 1. GPS map showing sample collection sites as thick dark spots

Materials and methods

Employed for this work are Energy Dispersive X-ray fluorescence spectrometer (MiniPAL4 ED-XRF), Scanning Electron Microscope (MVE016477830 SEM), X-Ray Diffraction (Empyrean XRD), and Fourier Transform Infra-red Spectrophotometer (Agilent tech. Cary 360 FTIR).

Sampling

Following documented protocol [6], 3 kg of the mineral ore samples were collected from 3 different pits and locations of the Yelwa Nono-Mbar, Bokkos mining sites of Plateau State. Samples were pretreated through washing, drying and grinding to particle size of 2 mm to distinguish between small and large particles. Agricultural soil samples were collected from mineral deposit vicinity (10-100 m) while samples for control experiment was collected from neighboring locations (300 – 500 m), from non-mine sites. The mineral and soil samples were identified at the National Metallurgical Development Center (NMDC) Jos, plateau state.

Physicochemical parameters of soil

Physiochemical parameters of the soil samples, including pH, conductivity and bulk density were carried out using documented standard laboratory procedures [7].

Ore characterization

SEM Analysis: SEM Phenomenon Prix model MVE016477830 was used for this analysis. Columbite and Tin samples were prepared using epoxy resins, polished and made conductive by carbon coating in a Dentom vacuum, DV-502A. The morphology of the Columbite and Tin ores were analyzed at an accelerating voltage of 20 KVA, real time of 21-36 and lifetime of 60 seconds. Images were made using the back scattering, electron detectors.

FTIR Analysis: The functional groups present in the Columbite and Tin ore samples were investigated using the furrier transform infra-red spectrometer. The mineral samples were ground and sieved employing a US standard test sieve with an ASTM E-11 speciation. Fourier Transform Infra-red Spectrometer (Agilent technologies Cary 360) was used for this analysis.

Energy Dispersive X-Ray Fluorescence Analysis: The EDXRF characterization methods based on the instruction manual and practiced by the National Metallurgical Development Centre NMDC was adopted. Optimum Efficiency Dry High-Intensity Magnetic Separator (Three Disc Rapid Magnetic Separator; 4-3-15 OG) was used in Beneficiating the Columbite and Tin ores respectively. 20.00 g of the ore samples was finely ground (beneficiated) to pass through a 200-250 mesh sieve. Depending on the nature of the sample, it was dried in an oven at 105°C for at least 1h and allowed to cool. The sample was intimately mixed with a binder in the ratio of 5.0 g sample(s) to 1.0 g cellulose flakes binder and palletized at a pressure of 10-15 tons/inch^2 in a pelletizing machine. At this stage the palletized sample(s) was stored in a desiccator for analysis. The ED-XRF (MiniPAL 4) was used to investigate the chemical composition of the soil, columbite and tin ore sample.

Soil pollution indices

Levels of pollution and degree of contamination was investigated using the Geo accumulation index and the contamination factor respectively. From eqn. 1, Bn is the average geochemical background values for each metal in columbite and tin samples, Cm is the percentage element in the oxide (measured total concentration of metals in soils) for agricultural soil samples around mining site and 1.5 is the background matrix correction factor due to lithogenic effects [8]. The geo-accumulation index (*Igeo*) is used to determine the level of soil contamination (Table 1). The I*geo* for heavy metal is calculated from base 2 logarithm of the measured total concentration of the metal over its background concentration as Eqn. (1):

$$I_{geo} = \log_2 (Cm/1.5Bn) \quad (1)$$

Analytical results were subjected to prescribed pollution indices. Contamination factor (CF) is channeled towards deriving a realistic estimate of the amount of contamination that impacts on the soil [10].

Modified degree of contamination (mCd) is used to calculate the degree of contamination of metals in soils [11]. It is given as Eqn. (2).

$$mC_d = \frac{1}{N}\sum_{i=1}^{N} CF_i \quad (2)$$

Table 1. Muller classification for geo-accumulation index [9]

I_{geo}	Class	Pollution status
>5	6	Extremely contaminated
4-5	5	Heavy to extremely contaminated
3-4	4	Heavily contaminated
2-3	3	Moderately to heavily contaminated
1-2	2	Moderately polluted
0-1	1	Uncontaminated to moderately contaminated
0	0	Practically uncontaminated

Where *N* is the number of elements to be analyzed and *CF* is the contamination factor calculated as shown in Eqn. (3).

$$CF = \frac{C_m Sample}{C_m Background} \quad (3)$$

X-ray diffraction (XRD) analysis

XRD analysis was carried out at the National Geoscience Research Laboratory (NGRL) Kaduna, Nigeria. The ores were exposed to air, allowed to dry and ground using a mechanical crusher. This was followed by sieving using sieve sizes ASTM 850 µm, 425 µm and 212 µm. Analysis of the samples was performed using Pan analytical (Empyrean model) X-ray diffraction machine. The samples were placed in a Lucite holder on the goniometer of the Scintag XDS 2000 powder diffractometer. It was also configured with a graphite monochromator and IBM compatible workstation running Scintag DMSNT software in a window NT environment. The diffraction beam monochromator operated at 20 KVA with step size of 0.02^0 for 120 minutes to create x- ray patterns with enough intensities so as to produce lines to identify minerals at the angles (5^0 – 100^0). The scanning rate was 0.75^0 per minute. Minerals were identified using the JCPDFWIN software. Peak analysis was also carried out using the Gaussian curve fitting. A continuous scan mode was used to collect 2θ data between 5.00° to 100° and the crystalline size was computed using the Debye-Scherrer equation given as Eqn. (4).

$$D = K\lambda/\beta \cos\theta \quad (4)$$

D is the mean ore diameter (Particle size), K is a constant with value 0.9, λ is the wavelength of X-ray (1.540598), β is full width at half maximum and θ is the differential angle [12].

Results and discussion

Physical inspection of samples

Figure 2 is a pictorial representation of sampling site and ore samples.

Mining vicinity was predominantly contaminated with mining waste called tailings.

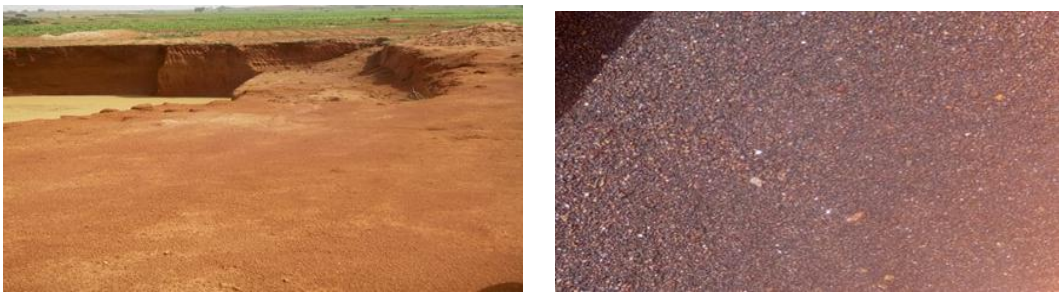

(A) (B)

Figure 2. Pictorial representation of Columbite -Tin mine site within farmland soil (LHS) and ore from study area (LHS)

The surrounding agricultural soil shows high tendency to leaching and erosion due to consistent mining activities and this was observed to have adverse effects on agricultural plants such as plants leaves coloration, Generally, the contamination of soils associated with mining operations by radionuclides and heavy metals leads to negative effect or influence on the soil characteristics and this limits production and environmental functions. Tailings have been found to contain high activity concentrations of ^{238}U and ^{232}Th and this could result in internal exposure of the entire living population through leaching activity which may be directly ingested through drinking water or may indirectly enter the food chain by uptake through vegetation, fish, milk and meat [3].

Physiochemical parameters of soil samples

Physiochemical parameters pH, conductivity and bulk density of agricultural soil samples around mine and control sites were quantified as 4.95, 0.05 (μS/cm) and 1.30 (g/cm^3) respectively. Their corresponding values for experimental control soil are 3.305, 0.035 (μS/cm) and 1.246 (g/cm^3).

pH: pH range of 3.3-5.0 was observed for agricultural soil samples. These pH values were lower than those observed in plants. Below pH 5.5, low legume and forage growth occur due to metal toxicities such as aluminum or manganese, phosphorus fixation, and reduced population of N-fixing bacteria. This growth, hence inhibits plant root growth and many other metabolic processes [14]. This result shows that pH of both sides was within the acidic range. Slightly higher value for the analytical soil sample could be linked to mining activities.

Bulk density: The density of the control sample (1.246 g/cm^3) is lower compared to that of the analytical soil sample estimated at 1.30 g/cm^3. This could result from

repeated traffic of wheeled mining machineries (loaders and haulers) forming compacted zones in the mining dumps. Report [15] shows that these values were slightly higher in clay soil. Generally, the bulk density of productive natural soils is 1.1 g/cm^3. High bulk density limits rooting depth in mine soils [16].

Conductivity: The mean conductivity value of the analytical soil sample ($0.07\mu S$/cm) and a control sample ($0.05\,\mu S$/cm) are generally llow. This may be linked to low level electrical potential in soils; clays and other water saturated and unsaturated sediments, few ionic layers, electro filtration, pH difference and electro osmosis [17].

SEM characterization of mineral ore

Figure 3 shows the morphological characteristics of the particles in the columbite and tin ores determined by SEM technique.

The surface morphology of the Tin and Columbite ores were examined using the scanning electron microscopy. It was earlier reported that cassiterite is the main ore mineral of tin occurring in the quartz veins of the plateau mining sites [18].

Investigating the surface morphology of the ore sample revealed a compact interlocking of these minerals within the irregular crystal aggregate of the ore sample. Figure 2 shows the typical SEM morphology of samples appearing in different sizes with irregular shapes showing compact aggregates at 150x magnification. Previous studies on nanocrystalline SnO_2 have shown that pure metastable tetragonal phase can be stabilized when the crystal size is below a critical size [19]. SEM assist in ore characterization and predictive metallurgy [18].

FTIR spectral characteristics

Spectral profile characteristics of each mineral samples (Figure 4) and their interpretation (Table 2) were presented.

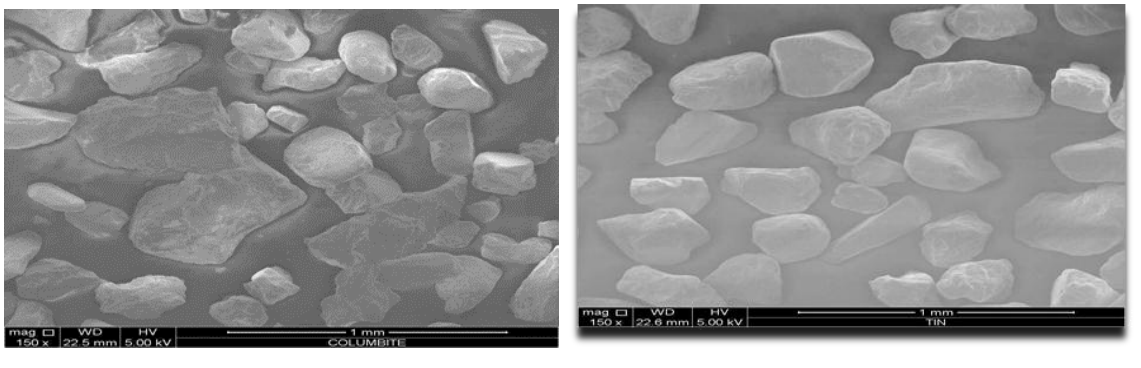

(A) (B)

Figure 3. SEM images of (a) Columbite and (b) Tin ores

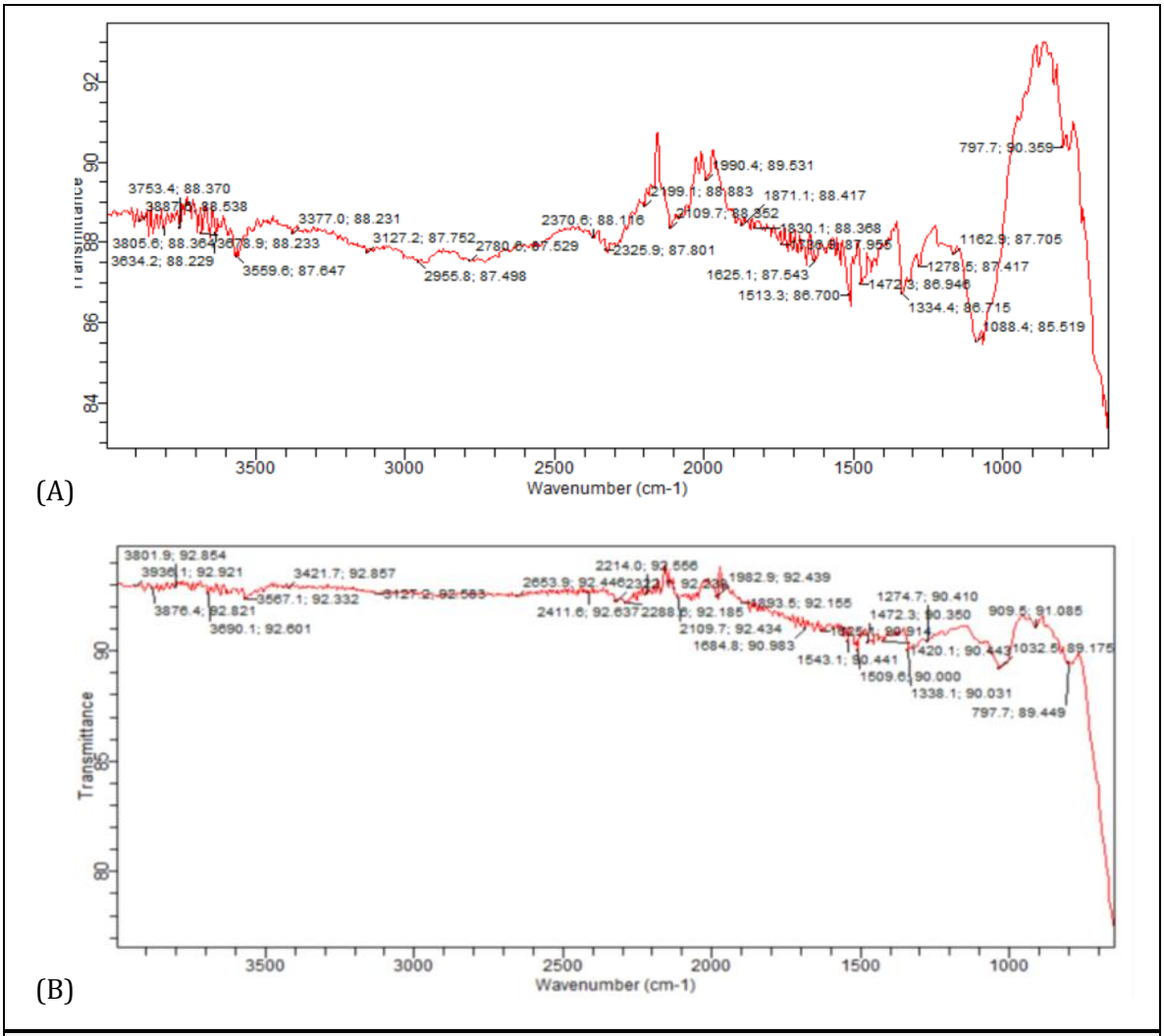

Figure 4. FTIR spectrum of Columbite (a) and Tin (b) ores

Table 2. FTIR spectral information of Columbite and Tin ore samples

Group freq. (cm^{-1})	Functional group	Observed frequency (cm^{-1}) Columbite ore	Tin ore	Assignment
797.7	Ag^{+}	797.7	797.7	Silver bromate
1100-1000	Ca^{2+}, Mg^{2+}	1088.4	-	Calcium phosphate and magnesium metaborate
1328-2380	Na^{+}	1334.4	1338.1	Sodium nitrate and related nitrate ions
1430-1640	Ca^{2+}, CO_3^{2-}	1472.3	1543.1	Calcium nitrate and carbonates
1560-1540	PO_4^{3-}	1513.3	1509.6	Calcium nitrate and carbonates
1555-1485/1355-1320	NO^{3-}	1162.9	-	Cyclic nitro compounds
2000-2200	CN^{-}, SCN^{-}	2325.9	2109.7	Cyanide ion, thiocyanide and related ions

The Fourier Transform Infrared (FTIR) Spectroscopy is an alternative method for acquiring quantitative and functional groups of mineral compounds [20]. From Figure 4. The absorption band range of 797.7 to 2200 cm^{-1} reveals the presence of compounds of Calcium phosphates and Magnesium metaborate, Silver bromate, Sodium nitrates, Calcium nitrates and Carbonates (Table 2). The carbonates spectra are characterized by strong absorption bands due to internal vibrational modes of the CO_3^{2-} groups [21]. The bands around 2935 cm^{-1} related to the total carbon present on the cell surface increased permanently. The spectra also revealed at the beginning of the process, for all tests, an increased number of anglesite and scontlandite bands [22]. The absorption bands reveal that Silver bromate, Nitrate ion, Ammonium phosphates and aliphatic Nitro compounds, Cyanides and Thiocyanide ions were present in the tin mineral ore, which are believed to be from the parent rock that form the surrounding soil [23].

X-ray fluorescence characterization of Columbite ore

Findings show that oxides of Silicon, Titanium, Chromium, Manganese, Iron and Zirconium have preferentially high percentage in Columbite sample compared to Tin sample. Oxides of Aluminum, Nickel, Zinc, Hafnium and Lead are detected in Columbite sample and were not detected in Tin sample. In the same vain, oxides of phosphorus and tungsten were detected only in Tin sample, while those of Silver, Bismuth and Thorium recovery were low in percentage for both Tin and Columbite samples. Table 3 presents the results of the chemical analysis of the columbite ore sample using electron dispersive XRF. The result revealed that the ore sample contained 2.20% Al_2O_3, 21.7% SiO_2, 19.59% TiO_2, 0.50% V_2O_5, 0.58% Cr_2O_3, 0.78% MnO, 26.73% Fe_2O_3, 0.11% ZnO, 0.93% Nb_2O_5, 0.17% Ta_2O_5, 0.83%SnO_2, 0.49% Ag_2O, 0.51% HfO_2, 0.27% ThO_2, 12.9% ZrO_2 and few of 0.05% CaO, 0.07% NiO, 0.09% PbO and 0.07% Bi_2O_3. Most of the Columbite mineral deposits in the Plateau mining sites are found to contain Niobium mineral. Available mineral depends on the geochemical composition of the minerals that formed the parent rock of the area [23]. This result also indicated that the ore cannot be utilized directly because of its low Niobium content unless it is beneficiated to meet metallurgical required grade. Thorium has a long half-life of 0.4×10^{10} years. It is used for making ceramics, welding rods, camera and telescope lenses, fire brick, heat

resistant paint, and metals used in the aerospace industry as well as a nuclear fuel [24]. It is evidence that breathing in thorium dust increases the risk of lungs and pancreatic cancer. Exposure to it also causes bone cancer because thorium can be stored in bone [25].

X-ray fluorescence characterization of tin ore

The result of the chemical analysis of the tin ore sample using ED – XRF as presented in Table 3 revealed that the ore sample contained 1.00% SiO_2, 0.63% P_2O_5, 2.86% cap, 2.03% TiO_2, 0.32% V_2O_5, 0.25% Cr_2O_3, 0.10% MnO, 2.35% Fe_2O_3, 1.85%Nb_2O_5, 0.49%Ta_2O_5, 85.43% SnO_2, 0.17% WO_3, 0.16% ThO_2, 0.85% ZrO_2, and low recovery percentages of 0.04% Ag_2O, 0.008% Bi_2O_3. The tin ore can be utilized directly in the furnace because of its high cassiterite (tin) content varying between deposit to deposit in the plateau mining sites.

Chemical composition of agricultural soil around mine site

XRF analysis was used to determine the chemical and percentage elemental composition of agricultural soil around mine site. This was presented in Table 3 revealing 12.40% Al_2O_3, 53.70% SiO_2, 0.08% P_2O_5, 0.60% K_2O, 0.38% CaO, 4.10% TiO_2, 0.16% V_2O_5, 0.31% CrO_3, 0.17% MnO, 18.22% Fe_2O_3, 0.01% NiO, 0.04% CuO, 0.03% ZnO, 0.02% Rb_2O, 2.60% ZrO_2, 0.37% Nb_2O_5, 0.11% ThO_2 and 0.03% Au were present in the sample. Concentrations of oxides of phosphorus, nickel and zinc are with contamination factor values of 0.18-1.0 mM, hence nontoxic [26]. However, Seeing the reoccurring hazards from mines across the Plateau state and other risks in the sector through inland sand mining and the effects of artisanal mining, the concentration of toxic residues, geological hazards and ecological disturbances and destruction of flora and fauna are major challenges from mining [27].

Results from Table 4 reveals that the oxides of Titanium, Iron, zirconium, Aluminum and silicon appears to be the most predominant oxides in both mineral ore samples and the mine site agricultural soil sample. Radionuclides such as potassium (K-40), Rubidium and Thorium were also present in the soil. The contamination of soils by radionuclides and heavy metals leads to a negative influence on soil characteristics and limits production and environmental functions. Thorium and phosphorus were not detected in the control sample. From this analysis, heavy metals and radioactive nuclides such as Al, Ca, Ti, V, Cr, Mn, Fe, Ni, Cu, Zn, Rb, Nb, and gold appears in very low concentrations compared to samples of agricultural soils around mining sites. These heavy metals are phytotoxic either at all

concentrations or above certain threshold levels [28].

Table 3. XRF result showing chemical composition of ores

S/No	Oxide	Composition of Oxide		Element	% element in oxide	
		Columbite (%)	Tin (%)		Columbite (%)	Tin (%)
1.	Al_2O_3	2.20	ND	Aluminum	8.154	NA
2.	SiO_2	21.7	1.00	Silicon	77.5	3.560
3.	P_2O_5	ND	0.63	Phosphorus	NA	2.034
4.	K_2O	ND	ND	Potassium	NA	NA
5.	CaO	0.05	2.86	Calcium	0.125	7.150
6.	SO3	ND	ND	Sulphur	NA	NA
7.	TiO_2	19.59	2.03	Titanium	40.89	4.238
8.	V_2O_5	0.50	0.32	Vanadium	0.982	0.628
9.	Cr_2O_3	0.58	0.25	Chromium	1.115	0.480
10.	MnO	0.78	0.10	Manganese	1.419	0.182
11.	Fe_2O_3	26.73	2.35	Iron	47.87	4.208
12.	NiO	0.007	ND	Nickel	0.012	NA
13.	CuO	ND	ND	Copper	NA	NA
14.	ZnO	0.11	ND	Zinc	0.168	NA
15.	Nb_2O_5	0.93	1.85	Niobium	1.001	1.991
16.	Ta_2O_5	0.17	0.49	Tantalum	0.094	0.270
17.	SnO_2	6.83	85.43	Tin	0.690	71.98
18.	WO_3	ND	0.17	Tungsten	NA	0.092
19.	Ag_2O	0.49	0.04	Silver	0.454	0.037
20.	HfO_2	0.51	ND	Hafnium	0.286	NA
21.	PbO	0.09	ND	Lead	0.043	NA
22.	Bi_2O_3	0.07	0.008	Bismuth	0.034	3.829
23.	ThO_2	0.27	0.16	Thorium	0.116	0.069
24.	ZrO_2	12.9	0.85	Zircon	14.14	0.932

ND-Not Detected, NA-Not Applicable

Table 4. XRF showing chemical composition of soil from mining and control sites

S/No	Oxide	% Oxides in Soil		Element	% element in Soil	
		Mine site (%)	Control (%)		Mine site (%)	Control (%)
1.	Al_2O_3	12.40	5.50	Aluminum	45.96	20.37
2.	SiO_2	53.70	78.98	Silicon	191.2	282.1
3.	MgO	ND	ND	NA	NA	NA
4.	P_2O_5	0.08	ND	Phosphorus	0.258	NA
5.	SO_3	ND	ND	NA	NA	NA
6.	K_2O	0.60	0.82	Potassium	1.534	2.097
7.	CaO	0.38	0.09	Calcium	0.950	0.225
8.	TiO_2	4.10	1.04	Titanium	8.559	2.171
9.	V_2O_5	0.16	0.03	Vanadium	0.314	0.059
10.	CrO_3	0.31	0.12	Chromium	0.596	0.230
11.	MnO	0.17	0.07	Manganese	0.309	0.127
12.	Fe_2O_3	18.22	4.80	Iron	32.62	8.595
13.	NiO	0.01	0.009	Nickel	0.017	0.015
14.	CuO	0.04	0.02	Copper	0.062	0.031
15.	ZnO	0.03	0.007	Zinc	0.046	0.011
16.	Rb_2O	0.02	0.01	Rubidium	0.023	0.012
17.	ZrO_2	2.60	0.40	Zircon	2.850	0.439
18.	Nb_2O_5	0.37	0.04	Niobium	0.398	0.043
19.	ThO_2	0.11	ND	Thorium	0.047	NA
20.	Au	0.03	0.02	Gold	0.015	0.010

ND-Not Detected, NA-Not Applicable

In the aquatic environment, these metallic elements or oxides gets into the streams through runoff of agricultural soils around mining sites existing in a number of different chemical forms (species), distributed between sediments and the solutions [29].

XRD characterization of columbite-tin mineral

Tables 5 present the crystallographic parameters of associated minerals and compounds in Columbite ore. Analysis was performed using X-ray diffraction technique. The diffractograms for compounds with Columbite ore are presented in Figure 5.

Mineralogy of columbite ore

The main minerals found in the Columbite sample were Braunite, Cassiterite, Ilmenite, Quartz, and Zircon. Each of these compounds has a phase information from the XRD pattern as shown in Figure 5 and Table 5. The diffraction of X-rays by the crystalline solid mineral sample results in a pattern of sharp Bragg reflections characteristic of the different d-spacing of the solid. Broadening of these reflections beyond that due to instrumental factors is generally attributed to crystallite size effects [30].

Braunite in columbite

This study revealed that the 2θ values of 32.982 and 55.317 shows high intensities (Table 6), and this is attributed to crystallite size effects. Braunite ($Mn_2O_3.MnSiO_3$) compound aside its occurrence alongside Columbite mineral, also occurs in regionally metamorphosed manganese deposits such as gondites and kodurites [31]. The occurrence of irregular zones of braunite around sand grains in manganiferous clays suggested that it was a reaction product possibly produced from the sedimentation of MnO_2 colloids.

Cassiterite in columbite

The 2θ values between 26.596, 33.875 and 51.785 reveals high intensities. Broadening of reflections beyond these values due to instrumental factors is attributed to crystallite size effects.

Table 5. Crystallographic parameters of columbite showing major compounds

S/No	Compounds	a (Å)	b (Å)	c (Å)	Alpha (^{0})	Beta(^{0})	Gamma (^{0})	Crystal system
1.	Braunite	9.4270	9.4270	18.695	90.0	90.0	90.0	Tetrahedral
2.	Cassiterite	4.7360	4.7360	3.1870	90.0	90.0	90.0	Tetrahedral
3.	Ilmenite	5.0832	5.0832	14.026	90.0	90.0	120	Hexagonal
4.	Quartz	4.9120	4.9120	5.4040	90.0	90.0	120	Hexagonal
5.	Zircon	6.5930	6.5930	5.9740	90.0	90.0	90.0	Tetragonal

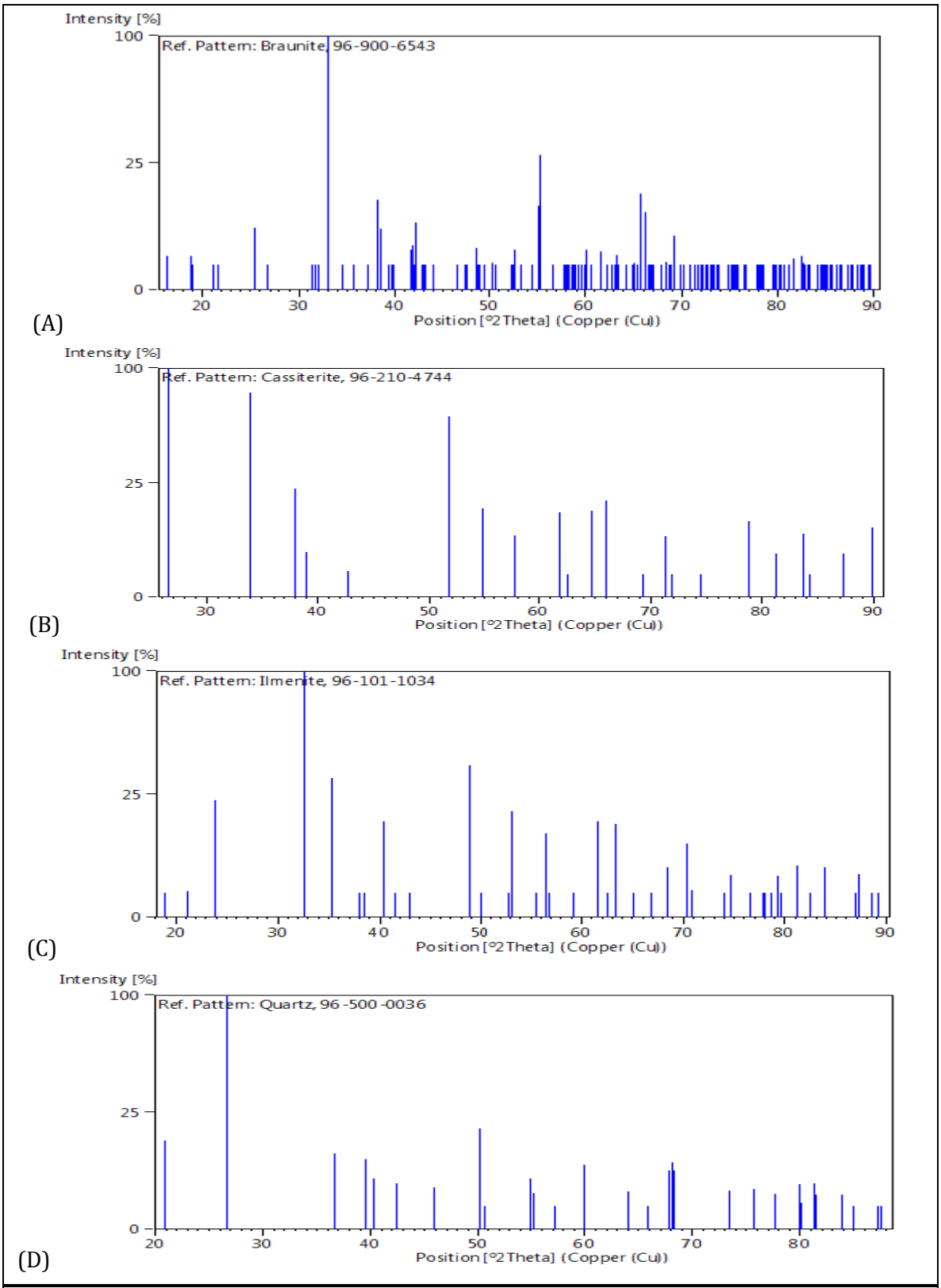

Figure 5. X-Ray diffractogram of (a) braunite (b) cassiterite (c) ilmenite and (d) quartz in columbite sample

Cassiterite is a typical wide band gap n-type semiconductor (3.6 Ev) and one of the widely used semiconductor oxides due to its chemical and thermal stabilities. It is a non-stoichiometric structure, and its conductivity mainly originates from the oxygen vacancies [32]. The electrical and chemical properties of cassiterite have been extensively studied, and this is because of its application as transparent electrodes for solar cell, liquid crystal display, anti-static coatings and gas sensors, anode for lithium ion batteries, transistors and as catalyst support [33].

Ilmenite in columbite

The chemical analysis of the Ilmenite in Columbite sample shows high intensity for 2θ at 32.622. Broadening of reflection attributed to crystallite size is less. Ilmenite ($FeTiO_3$) is black and opaque with TiO_2 contents between 45 and 65% usually occurring alongside other sand minerals such as tin and columbite. Because it is non-toxic, it is used in cosmetics and pharmaceuticals. About 6% is used to manufacture titanium metal, a light, strong, corrosion-resistant metal used in aircraft, spacecraft and medical prostheses. Its application in the process of fine grain materials aggregation or pelletizing cannot be over emphasized [34].

Quartz in columbite

Quartz has also revealed a single high intensity at 2θ value 23.647, other intensities reveal lower values below 25% intensity. Broadening of these reflections beyond that due to instrumental factors is attributed to crystallite size effects. Quartz sand is the final product of rock weathering which is an important part of the rock cycle. On the Jos plateau, quartz is the major component of the abundant rock minerals in the state. The weathering of any quartz-bearing rock creates sand: igneous, sedimentary, or metamorphic rocks. Quartz is used in a great variety of products and the term "quartz sand" in its finest form, as micro-silica it is used as an essential raw material for the glass and foundry casting industries, as well as in other industries such as ceramics, chemical manufacture and for water filtration purposes.

Zircon in columbite

The result revealed that the 2θ values for Zircon (20.041, 27.027, 35.670 and 53.560) shows high intensities. This implies that broadening of reflections beyond 25% due to instrumental factors is predominant for zirconium in columbite sample and this is also attributed to crystallite size effects. Zircon (ZrSiO4); Zirconium silicate, often occurs with some hafnium (1 to 4 %.) and occasionally with solid minerals such as tin, uranium, Columbite, Hafnium, thorium, and yttrium [26]. Zircon sand is used in various range of industrial applications and in a variety of markets ranging from foundry molding sands to zirconium-metal manufacture. This analysis shows that zircon

occurs alongside radioactive elements such as U and Th [25].

Mineralogy of tin ore

The mineralogy of the crushed Tin ore was carried out by X –ray diffraction technique. The main minerals found in the sample were Cassiterite, Litharge and Magnetite, with each of this compound having a phase information from the XRD pattern. In the plateau mining sites, Tin occurs naturally in the form of cassiterite with varying amounts of associated minerals [6]. The principal minerals of commercial interest are Titanium Minerals (rutile and Ilmenite), columbite (niobium and tantalum), Monazite, magnetite, litharge, and zircon. Cassiterite main use is in bronze alloy and as a component in low-melting solder with antimony and lead [6].

Pollution study

Table 7 presents the level of contamination at the mine-site and the control site soil while Table 8 shows the **Geo** accumulation index (I_{geo}) of farmland soils. Pollutants with high Contamination factors, CF >2 are Cr, Mn, Fe, Ti, V, Al. Niobium (9.255) and Zircon (6.492) are more predominant. According to prediction by I_{geo} index, high level pollutants beside tin, are aluminum, titanium, iron and zircon. They fell within the range of moderately to heavily contaminated [9].

Table 6. XRD peak information of braunite in columbite sample

S/No.	d [Å]	2 Theta [deg]	I [%]	Crystalline size(nm)
1.	3.49186	25.488	6.0	0.0171
2.	2.71363	32.982	100.0	0.0184
3.	2.35675	38.155	12.6	0.0196
4.	2.33687	38.492	5.8	0.0197
5.	2.14268	42.139	7.1	0.0208
6.	1.66647	55.063	11.0	0.0269
7.	1.65940	55.317	28.1	0.0271
8.	1.42007	65.699	14.5	0.0374
9.	1.41135	66.158	9.5	0.0381

Table 7. Contamination factor C_f of elements in columbite-tin soil

Class	Elements	% Composition		C_f
		Mine site	Control	
Heavy metals	Manganese	0.309	0.127	2.433
	Chromium	0.596	0.230	2.591
	Iron	32.62	8.595	3.795
	Titanium	8.559	2.171	3.942
	Vanadium	0.314	0.059	5.322
Non-essential	Zircon	2.850	0.439	6.492
	Niobium	0.398	0.043	9.255
	Aluminum	45.98	20.37	2.257
	Gold	0.015	0.010	1.500
Non metal	Phosphorus	0.258	ND	0.258
	Silicon	191.2	282.1	0.677
Radionuclides	Potassium	1.534	2.097	0.731
	Rubidium	0.023	0.012	1.916
	Thorium	0.047	ND	0.047

Table 8. Pollution load as geo accumulation index (I_{Geo}) of farmland soils

Element	Bn	Cm	I_{geo}	Pollution status
Aluminum	8.154	45.96	2.397	Moderately contaminated
Silicon	40.513	191.2	3.713	Heavily contaminate
Calcium	3.6375	0.950	0.362	Uncontaminated
Titanium	22.564	8.559	2.109	Moderately contaminated
Vanadium	0.805	0.314	-0.773	Uncontaminated
Chromium	0.797	0.596	-0.499	Uncontaminated
Manganese	0.801	0.309	-0.782	Uncontaminated
Iron	26.03	32.62	2.753	Moderately contaminated
Nickel	0.012	0.017	-.3.866	Uncontaminated
Zinc	0.168	0.046	-.20288	Uncontaminated
Niobium	1.496	0.398	-0.401	Uncontaminated
Thorium	0.093	0.047	-2.537	Uncontaminated
Zircon	7.536	2.850	1.155	Moderately contaminated
Phosphorus	2.034	0.258	-0.456	Uncontaminated

Conclusion

The results obtained in the mineralogical characterization of Columbite-Tin ore and their vicinity agricultural soil confirm the presence of mineral elements, trace metals and radionuclides in farmland soils around Columbite-Tin mining sites. XRD characterization uncovered the presence of associated minerals, notably braunite, cassiterite, ilmenite, quartz, and zircon in columbite while cassiterite, magnetite and litharge were traced in tin mineral. The chemical composition indicates that the over eighteen (18) stable and radioactive elements present in the mineral ores were also found in the vicinity agricultural soil. Both the geo-accumulation and contamination factor indices present some level of pollution. These elements were linked to different forms of soil deconditioning. Of great concern is the presence of Radionuclides K-40, Rubidium and Thorium in the soil. The contamination of this soil by radionuclides and other heavy metals could lead to a negative influence on soil characteristics and limits production and environmental functions. From the highlights of this research, it is recommended that mining operations should be carried out under strict environmental laws and regulations to forestall agricultural farmlands contamination and the introduction of safe mining practices coupled with advanced technology are needful for heath consideration and exploitation of associated minerals respectively.

ORCID

A.U. Itodo : 0000-0002-4755-2270

References

[1]. S.U. Onwuka, J.O. Duluora, C.O. Okoye,

Int. j. Eng. Sci. invent., **2013,** *2*, 30-34.

[2]. A.O. Adegbulugbe, *Int. J. Eng. Sci. Invent.,* **2007***, 2*, 2319 – 6734.

[3]. S.S. Ahluwalia, D. Goyal, *Biores. Technol. J.,* **2007**, *98*, 2243–2257.

[4]. S.J. Mallo, *the Nigerian Mining Journal*, 1999, **3**, 1-2.

[5]. M.A. Adeniran, E. Ekpo , O.A, Adedayo, V.J, Ibekwe, case study of Jos metropolis, Plateau state, Nigeria. **2013**, *1*, 1-3

[6]. M. Klementova, M. Rieder, Z. Weiss, *J. GEOsci*. **2000**, 45, 155-157.

[7]. M. Ahmedna, W.E. Marshall, R.M. Rao, *Biores. Technol.,* **2000***, 71*, 113-123.

[8]. E.E. Ntekim, S.J. Ekwere, E.E. Ukpong, *Environ. Geol.,* **2015**, *4*, 237-241.

[9]. W. Wang, G. Yang, I.A. Pablo, L. Anxin, *Geomorphorlogy*, **2015**, *1*, 1-7

[10]. J.L. Schroeder, N.T. Basta, S.W. Casteel, T. Evans, T.J. Payton, J. Si, *J. Environ. Quality,* **2004**, *33*:513–521.

[11]. P.W. Abraham, *Sci. Total Environ*., **2002**, 29, **1**, 1-32

[12]. H.U. Itodo, L.A. Nnamonu, R.A. Wuana, *Asian J. Chem. Sci.* **2017**, *3*, 1-10.

[13]. N.N. Jibiri, I.P. Farai, I.S.K. Alausa, *Int. J. Soil, Sediment and Water*, **2007**, *2*, 7-10.

[14]. V. Sheoran, A.S. Sheoran, P. Poonia, *Int. J. Miner. Process.*, **2010**, *6*, 1-19.

[15]. P. Koorevaar, G. Menelik, C. Dirksen, *Elements of soil physics (vol.13)*, Elsevier, **1983**, pp. 1-12.

[16]. S.K. Maiti, M.K. Ghose, Nigeria, *J. Radiol. Prot.,* **2005**, *28*, 93-99.

[17]. A.I. Pozdnyakova, L.A. Pozdnyaakova, *J. Environ. Sci*., **2002**, *7*, 14-21.

[18]. M. Ogwuegbu, G. Onyedika, J.Y. Hwang, A. Ayuk, Z. Peng, B. Li, E.N.O. Ejike, M. Andriese, *J. Miner. Mater. Characterizat. Eng.*, **2011**, *10*, 855-863.

[19]. A. Ayeshamariam*,* C. Sanjeeviraja, R.P. Samy, *J. Photon. Spintron.,* **2013**, *2***,** 4-9*.*

[20]. N.J. Cook, *Norg. Geol. Unders. B.,* **2000***, 438*,189-192.

[21]. P. Patra, K.A. Natarajan, *J. Coll. interface Sci.*, **2006**, *298*, 720 – 729.

[22]. P.K. Sharma, R.K. Hanumantha. *Miner. Metal. Process*. **2005**, *22*, 31.

[23]. D.G. Thomas, F. Asuke, S.A. Yaro, *Proceedings of the Nigeria Engineering Conference, Faculty of Engineering,* **2014**, 827-841.

[24]. E.A. Casartelli, N. Miekeley, *Anal. Biol. Chem. J.,* **2003**, *377*, 58–64.

[25]. C. Peng, Y. Ma, Y. Ding, X. He, P. Zhang, T. Lan, D. Wang, Z. Zhang, Z. Zhang, *Int. J. Mol. Sci*., **2017**, *18*, 795.

[26]. B.E. Allred, P.B. Rupert, S.S. Gauny, D.D. An, C.Y. Ralston, M. Sturzbecher-Hoehne, R.K. Strong, R.J. Abergel, *Proc Natl Acad Sci U S A.,* **2015***,* 112, 10342

[27]. M.S. Chanada, N.G. Obaje, A. Moumouni, N.G. Goki, U.A. Lar, *Online J. Earth Sci.,* **2010**, 4, 38-42.

[28]. K. Pollard, C. Rickaby, M. Miers, *Health Sciences and Practice,* **2008***,* 77-78.

[29]. O. Zmora, D.J. Grosse, N. Zou, T.M. Samocha, Microalgae for aquaculture: practical implications. *Handbook of microalgal culture. Wiley, Chichester*, **2013**, pp. 628-652.

[30]. S. Britto, S. Joseph, P.V. Kamath, *J. Chem. Sci*., **2010**, *122*, 751–756

[31]. M. Roy, C.D. Hirak, *Neues Jahrb. Mineral,* **1981**, *142*,149-160.

[32]. B. Yang, X. Zhong, X. Zhang, J. Jia, G. Yi, *Particuol. J.,* **2012**, *10*, 365-370.

[33]. G. Du, C. Zhong, P. Zhang, Z. Guo, Z. Chen, H. Liu, *Electrochim. Acta,* **2010**, *55*, 2582-2586.

[34]. T. Inada, A. Kasai, K. Nakano, S. Komatsu, A. Ogawa, *ISIJ Int.,* **2009**, 49, 470-478.

How to cite this manuscript: Adams Udoji Itodo*, Raymond Ahulle Wuana, Bulus Emmanuel Duwongs, Davoe Danbok Bwede, Mineralogy and Pollution Status of Columbite-Tin Ore Contaminated Soil*, Adv. J. Chem. A*, **2019**, *2*(2), 147-164.